SIAM J. APPL. MATH.
Vol. 61, No. 3, pp. 792–802

ELECTRODIFFUSION MODEL OF RECTANGULAR CURRENT PULSES IN IONIC CHANNELS OF CELLULAR MEMBRANES*

CARL L. GARDNER†, JOSEPH W. JEROME‡, AND ROBERT S. EISENBERG§

Abstract. A simplified electrodiffusion model for rectangular current pulses in ionic channels of biological membranes is presented. Numerical simulations and a dynamical systems analysis of traveling wave solutions in the model indicate that the durations and separations of current pulses vary stochastically in time, as is observed experimentally. An electrodiffusion theory of the mechanism for gating is advanced.

Key words. electrodiffusion model, ionic channels, dynamical systems

AMS subject classifications. 76Z99, 92C05

PII. S0036139999351645

1. Introduction.

Ionic channels are the main pathway by which the cell communicates—by exchanging substances and electric charge—with its environment. Channels are responsible for signaling in the nervous system, for coordination of muscle contraction (including the pumping action of the heart), and for ionic transport in every cell and organ. A substantial fraction of all drugs employed by physicians act directly or indirectly on ionic channels.

Ionic current pulses have been observed experimentally in a wide variety of channels in the membranes of many types of cells (see [1] and references therein). These current pulses are of rectangular wave shape with constant height and are distributed stochastically in time. In this investigation we demonstrate the existence of stochastic-in-time rectangular current pulse traveling waves for a simplified electrodiffusion model of the biological channel developed in analogy with the Gunn diode in semiconductor physics.

We consider a flow of positive ions (cations) in a one-dimensional channel in an electric field $E(x,t)$ against a background of negatively charged atoms on the channel protein ("doping" in the semiconductor context). The discrete distribution of charges is described [2, 3, 4] by continuum particle densities $p(x,t)$ for the mobile cations and N for the negatively charged atoms of the protein. We will allow N to be a function of current density and electric field, but not explicitly of x or t. The flow of cations is modeled mathematically by the drift-diffusion (Poisson–Nernst–Planck) model, that is, by a partial differential equation for conservation of the cations and Gauss's law for the electric field, plus a constitutive law specifying the current density $j(x,t)$:

$$\frac{\partial p}{\partial t} + \frac{1}{e}\frac{\partial j}{\partial x} = 0, \tag{1}$$

*Received by the editors February 5, 1999; accepted for publication (in revised form) April 26, 2000; published electronically September 7, 2000.
http://www.siam.org/journals/siap/61-3/35164.html

†Department of Mathematics, Arizona State University, Tempe, AZ 85287-1804 (gardner@asu.edu). The research of this author was supported in part by the National Science Foundation under grant DMS-9706792 and by DARPA under grant N65236-98-1-5409.

‡Department of Mathematics, Northwestern University, Evanston, IL 60208 (jwj@math.nwu.edu). The research of this author was supported in part by the National Science Foundation under grant DMS-9704458.

§Department of Molecular Biophysics and Physiology, Rush Medical College, Chicago, IL 60612 (beisenbe@rush.edu). The research of this author was supported in part by DARPA under grant N65236-98-1-5409.

$$\frac{\partial}{\partial x}(\epsilon E) = e^2(p - N), \tag{2}$$

$$j = \mu p E - eD\frac{\partial p}{\partial x}, \tag{3}$$

where e is the proton charge, ϵ is the dielectric coefficient (taken here to be constant), μ is the mobility coefficient, and D is the diffusion coefficient. The usual electric field has been multiplied by e (i.e., E has units of eV/cm in the cgs system). Typically, in semiconductors both μ and D depend on E.

Periodic and single-pulse (homoclinic) traveling wave solutions [5] for charge density and electric field—and thus for current—are obtained for the Gunn diode when the mobility $\mu(E)$ exhibits negative differential conductance, a region on the current-voltage curve where the current *decreases* as the voltage is increased. (In fact, dynamical oscillatory behavior in the Gunn diode occurs for a wide class of models; e.g., the two valley hydrodynamic model produces this behavior [6].) In the biological channel setting, μ and D are believed to be very nearly constant for relevant values of E. However, if the charge distribution N on the protein is allowed to depend on current density and electric field—because the protein conformation changes—then rectangular traveling wave current pulses exist in the drift-diffusion model. These traveling waves in p and E preserve their shape and propagate with constant velocity by balancing drift effects against diffusion.

We will follow Szmolyan's analysis [5] closely through (6) and (7) below. The drift-diffusion equations for traveling wave solutions are first put into scaled form and integrated once. Then the existence of stochastic-in-time rectangular current pulses for a model $N = N(j, E)$ with noise will be demonstrated.

2. Drift-diffusion model for traveling waves. To find traveling wave solutions, we set $s = x - v_0 t$ and look for solutions p and E that depend only on s. The traveling wave velocity v_0 is a free parameter and turns out to be on the order of the ion permeation velocity through the channel. The drift-diffusion equations (1)–(3) become

$$-ev_0\frac{dp}{ds} = \frac{d}{ds}\left(-\mu p E + eD\frac{dp}{ds}\right), \tag{4}$$

$$\frac{dE}{ds} = \frac{e^2}{\epsilon}(p - N). \tag{5}$$

Equation (4) can be immediately integrated to yield the following scaled equations:

$$\alpha\frac{dp}{ds} = p\left(E - \overline{E}\right), \tag{6}$$

$$\frac{dE}{ds} = \frac{e^2}{\epsilon}(p - N) \equiv \frac{e}{\epsilon}\rho, \tag{7}$$

where $\alpha = eD/\mu$ and $\overline{E} = ev_0/\mu$. The constant of integration in (6) is set to zero by requiring that dp/ds and $dE/ds \to 0$ as $t \to \pm\infty$ and $E(t \to \pm\infty) = \overline{E}$, in other words, by requiring that the solution (p, E) goes to a fixed point as $t \to \pm\infty$.

For traveling wave solutions the current density is simply proportional to the cation density:

$$j = \mu \left(pE - \alpha \frac{dp}{ds} \right) = ev_0 p. \tag{8}$$

The charge density $\rho = e(p - N)$ in Gauss's law (7) will, in general, depend on the current and the electric field. For the traveling wave solutions we will consider $\rho = \rho(p, E)$ due to (8).

We know from experimental observations that there is a "rest" value $\overline{E}$ of the electric field at which the current is constant—either "on" at a value $j_+ \equiv ev_0 p_+$ or "off" at a value $j_- \equiv ev_0 p_- \ll j_+$, where the subscripts + and − denote, respectively, the on and off state values. The rest values of the electric field for the on and off states must be the same because of charge conservation: by Gauss's law,

$$\int_{x_-}^{x_+} \rho \, dx = \frac{\epsilon}{e} (E_+ - E_-) = 0 \tag{9}$$

only if $E_+ = E_-$; $E_- \neq 0$ since even in the off state there is a nonzero "built in" potential difference across the cell membrane and thus a nonzero electric field. Here x_+ and x_- are locations where the current is, respectively, on or off. The integral of the charge density from the off to the on state must vanish for the traveling wave, since otherwise an enormous electric field would develop and cause a spark discharge across the cell membrane, destroying the cell, in contradiction to what is observed in nature. Similar remarks apply when integrating from the on to the off state.

The drift-diffusion traveling wave equations mirror this rest-state property since for $E = \overline{E}$ equation (6) implies p and hence j is constant, and (7) is satisfied if $\rho(p_\pm, \overline{E}) = 0$.

Further, to produce symmetrical rectangular current pulses as solutions to (6) and (7), the charge density in Gauss's law must be an even function of $E - \overline{E}$. This symmetry property is manifest in Figure 1 ($\overline{p}$ is a reference ion density defined through (10)) and follows from the invariance of the drift-diffusion traveling wave equations (6) and (7) under the transformation $p \to p$, $dp/ds \to -dp/ds$, $E - \overline{E} \to -(E - \overline{E})$, and $dE/ds \to dE/ds$. The reader may check that for a pulse in ion density, the electric field must consist of two equal and opposite spikes because of (6). This symmetry then implies that ρ must be an even function of $E - \overline{E}$.

A simple, physically based model with these properties which produces rectangular current pulses is

$$\rho(p, E) = -ce(p - \overline{p}) \left| \frac{E}{\overline{E}} - 1 \right|, \tag{10}$$

where $c \ll 1$ is a positive constant and $\overline{p} > 0$ is a reference ion density at which the slope of E reverses sign. Note that our model has $\rho(p, \overline{E}) = 0$ for all p—which produces a line of fixed points for the drift-diffusion traveling wave equations—and is a stronger condition than the constraint above that $\rho(p_\pm, \overline{E}) = 0$. See [7] for the characterization of a line of fixed points in terms of the vanishing of $\rho(p, \overline{E})$ for all p.

The charge density (10) can be derived from a Boltzmann factor. The energy per unit time required to create a current perturbation $\delta\mathbf{j}$ in an electric field $\mathbf{E}$ is $dU/dt = -\int \delta\mathbf{j} \cdot \mathbf{E} \, d^3x$ (see, e.g., [8, Chapter 27]). We will modify the expression for U to take into account that no work is done in the channel when $E = \overline{E}$ and that the

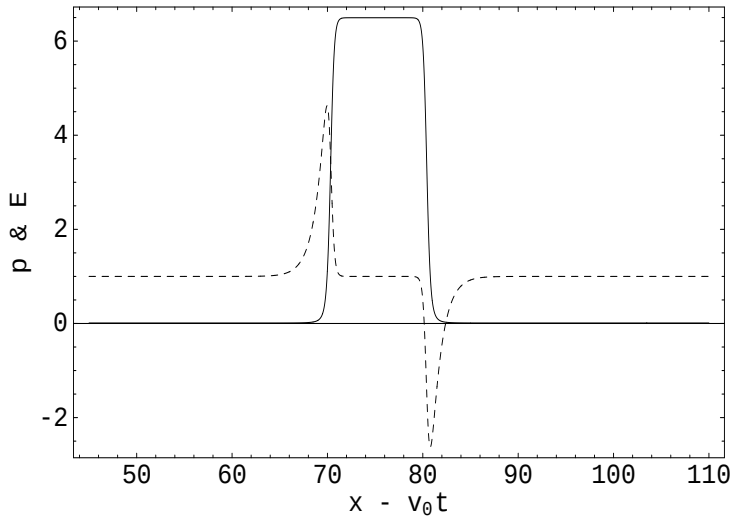

FIG. 1. *Traveling wave solution consisting of a rectangular current pulse* $p/\overline{p} \propto j$ *(solid line) and electric field* $E/\overline{E}$ *(dotted line) vs.* $(x - v_0 t)\overline{E}/\alpha$.

current perturbation $\delta j = ev_0(p - \overline{p})$ is with respect to $ev_0\overline{p}$. Then the energy per unit time to turn on a current pulse by creating δj is

$$U_{on} = -v_0(p - \overline{p})(E - \overline{E})A_C\delta x\delta t, \tag{11}$$

where A_C is the cross-sectional area of the channel and δx and δt are length and time scales over which the current perturbation turns on or off. Note that a factor of e has been incorporated into our definition of the electric field. To turn off a current pulse by destroying δj, the energy per unit time is

$$U_{off} = -U_{on} = v_0(p - \overline{p})(E - \overline{E})A_C\delta x\delta t. \tag{12}$$

Since $E - \overline{E} > 0$ when the current pulse is turned on (see Figure 1) and < 0 when the current pulse is turned off, we can write U as

$$U = -v_0(p - \overline{p})|E - \overline{E}|A_C\delta x\delta t. \tag{13}$$

Thus, in our model only the magnitude of displacements of E from $\overline{E}$ matters.

We assume that near thermal equilibrium $p \approx \overline{p}$ and that N is governed by a Boltzmann factor

$$N \approx \overline{p}\exp\{-U/(kT_0)\}, \tag{14}$$

where kT_0 is the ambient temperature in energy units. Near thermal equilibrium, the charge density in the channel is

$$\rho \approx e\overline{p} - e\overline{p}\exp\{v_0(p - \overline{p})|E - \overline{E}|A_C\delta x\delta t/(kT_0)\}$$

$$\approx -ce(p - \overline{p})\left|\frac{E}{\overline{E}} - 1\right|. \tag{15}$$

Note that the electric field term in ρ has the required even symmetry in $E - \overline{E}$. With the parameter values chosen below in section 4 to model a K^+ channel, δx turns out to be on the order of 0.2 Å and δt on the order of 10 nanoseconds—which are physically plausible values over which the current perturbation might turn on or off.

We will also add a random noise term σ, representing small charge density fluctuations, to the right-hand side of Gauss's law. We set σ equal to $+\overline{\sigma}$, 0, or $-\overline{\sigma}$, where $\overline{\sigma} \ll 1$ is a positive constant. The nonzero values of σ are randomly distributed with uniform probability in time with zero mean, i.e., with equal probability of being positive or negative. Generating noise $\pm\overline{\sigma}$ with zero mean guarantees charge conservation.

We control the frequency of noise by generating a random number r using the C library function random( ) at each timestep and comparing r with a fixed number $R \in [0, 1]$ which sets the specified frequency. If $r \geq R$, then we set $\sigma = \pm\overline{\sigma}$, where the sign is chosen randomly. If $r < R$, we set $\sigma = 0$. Thus if $R = 0.999$, noise is added on the average once every thousand timesteps.

The magnitude $\overline{\sigma}$ should be chosen small enough so as not to visibly affect the height of the current pulses over the course of the simulation (see section 3 below), since these heights are constant to very high accuracy in the experimental data. As long as this condition holds, plots of the computed solutions do not differ visibly with the magnitude of $\overline{\sigma}$. This model for noise generation mimics thermal fluctuations of charge density (where $\overline{\sigma}$ corresponds to the average of the absolute value of the thermal fluctuations), since it is the *existence* of small thermal fluctuations of charge density that is important, and not their quantitative magnitude.

The drift-diffusion equations can now be written as

$$\frac{dp}{d\tau} = p\left(E - \overline{E}\right), \tag{16}$$

$$\frac{dE}{d\tau} = -\overline{c}(p - \overline{p})\left|\frac{E}{\overline{E}} - 1\right| + \sigma(\tau), \tag{17}$$

where $\tau = s/\alpha$ and $\overline{c} = \alpha e^2 c/\epsilon$.

The traveling wave equations (16) and (17) without noise are integrable:

$$E = E_0 \pm \overline{c}(p - p_0 - \overline{p}\ln(p/p_0))/\overline{E}, \tag{18}$$

where the initial conditions are $p(\tau = 0) = p_0$ and $E(\tau = 0) = E_0$. Equation (18) may be used to plot phase space orbits.

3. Simulation of rectangular current pulses. Without noise, the differential equation system (16) and (17) has a line of fixed points at $E = \overline{E}$ (see Figure 2). The orbit is heteroclinic since there are two fixed points per orbit. A small amount of noise σ—presumably due to thermal fluctuations of charge density—in Gauss's law is sufficient to perturb the solution off the fixed points. Since the orbit slows down in the vicinity of the equilibria, the solution will spend most of the time near the maximum or minimum values of p, producing rectangular current pulses. By varying the initial conditions p_0 and E_0, a nested set of heteroclinic orbits is mapped out in phase space. The noise term σ can knock a trajectory from one orbit to another nearby orbit. We take $\overline{\sigma}$ small enough so that the maximum value of p over an orbit remains constant to six significant figures even over 100,000 orbits.

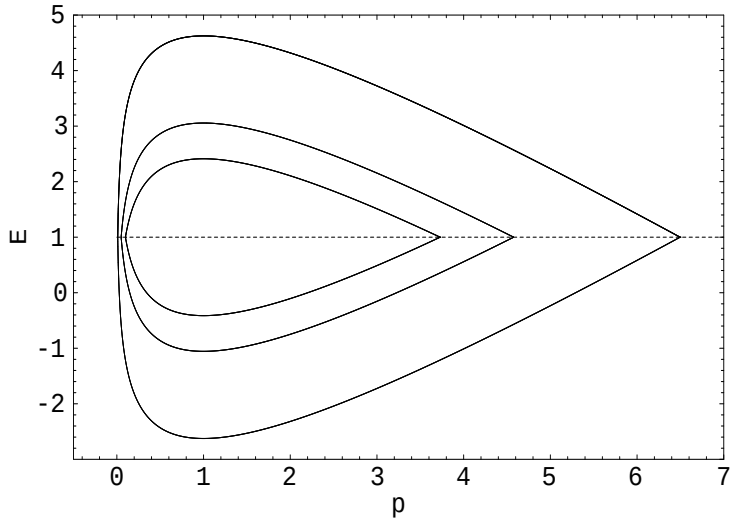

FIG. 2. *Heteroclinic orbits in phase space* $(p/\overline{p}, E/\overline{E})$ *for different initial conditions* p_0, E_0. *The line of fixed points is also shown.*

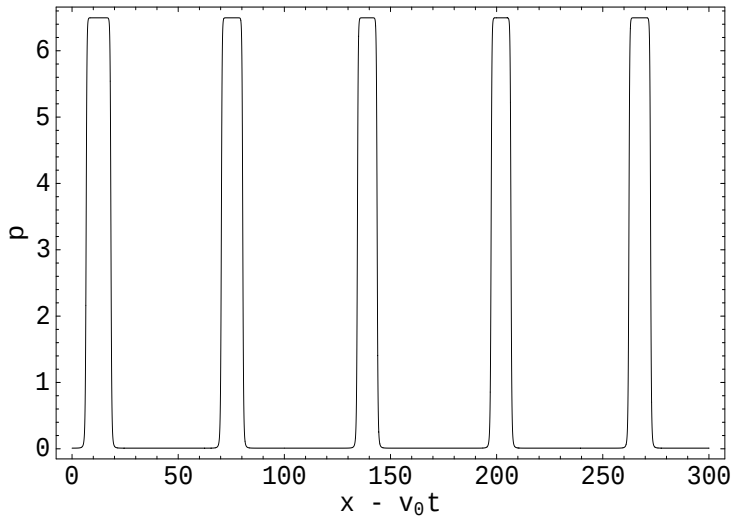

FIG. 3. *Solution* $p/\overline{p}$ *vs.* $(x - v_0 t)\overline{E}/\alpha$ *with random noise added every timestep.*

In Figures 3 and 4 we display the solution with noise added every timestep for $p(\tau)$ and total charge density ρ, with $p_0 = 0.01\overline{p}$, $E_0 = 1.01\overline{E}$, $\bar{c} = \overline{E}^2/\overline{p}$, and $\overline{\sigma} = \pm 10^{-9}\overline{E}^2$. Recall that the current density $j(\tau) \propto p(\tau)$ and that the integral of the charge density as the current pulse turns on or off vanishes (preserving charge neutrality). Also note that the physical charge density will be multiplied by $c \ll 1$, ensuring that the charge density is small in magnitude compared with $\overline{p}$.

The solutions are computed from (16) and (17) (and have converged under timestep refinement) using a fourth-order Runge–Kutta method with a fixed timestep $\Delta t = 0.01$ chosen to guarantee that the local truncation error is always less than 10^{-9}. (A fixed timestep is necessary in order to control the frequency of noise. In addition, the

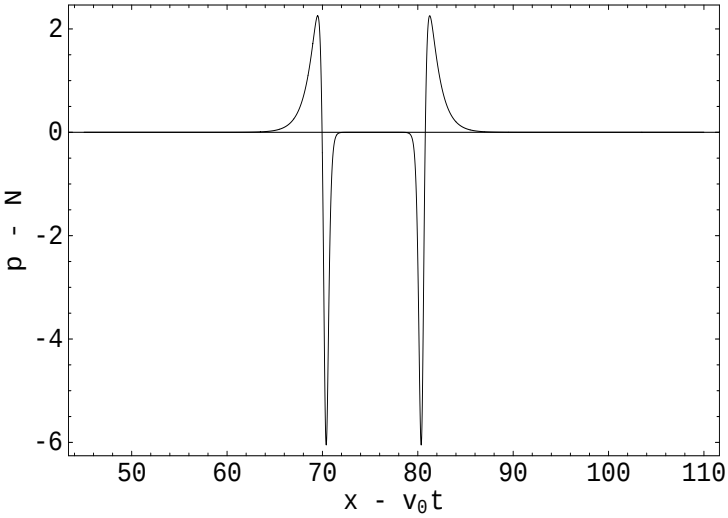

FIG. 4. *Charge density* $(p-N)/(c\overline{p}) \sim 10^6(p-N)/\overline{p}$ *vs.* $(x-v_0t)\overline{E}/\alpha$.

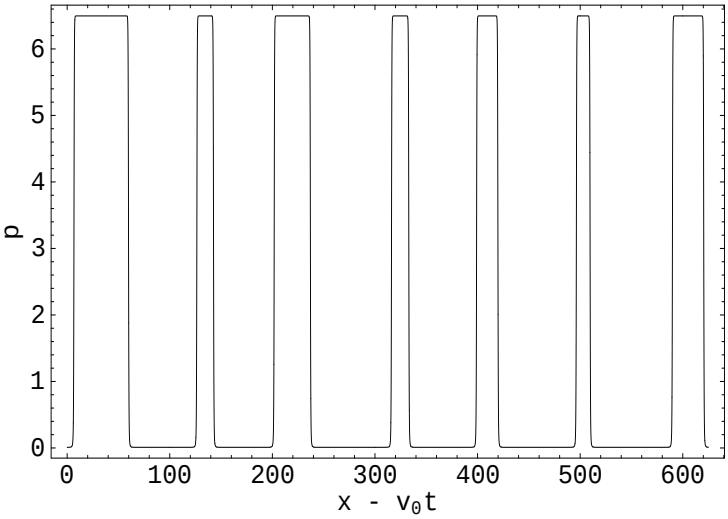

FIG. 5. *Solution* $p/\overline{p}$ *vs.* $(x-v_0t)\overline{E}/\alpha$ *with random noise added every thousandth timestep on average.*

simulations ensure that the point $E = \overline{E}$ is not jumped over.) The horizontal axis $x - v_0t$ in the figures may be interpreted at fixed t as space running to the right or at fixed x as time running to the left.

The durations and separations of the current pulses vary over a wide range (see Figures 5 and 6), as is observed experimentally. This wide variety of current pulse durations and separations is obtained by making the noise term in (17) more or less frequent. These simulations represent specific *realizations* of solutions to (16) and (17). By changing the seed of the random number generator for the noise term σ, we obtain other realizations. A histogram of the number of pulses versus pulse duration for a time period of 250 seconds (using the parameter values below in section 4) is presented

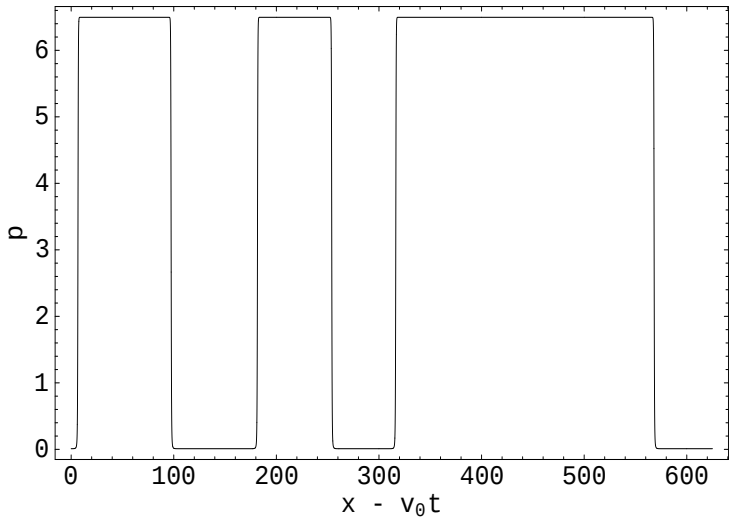

FIG. 6. *Solution $p/\overline{p}$ vs. $(x - v_0 t)\overline{E}/\alpha$ with random noise added every ten thousandth timestep on average.*

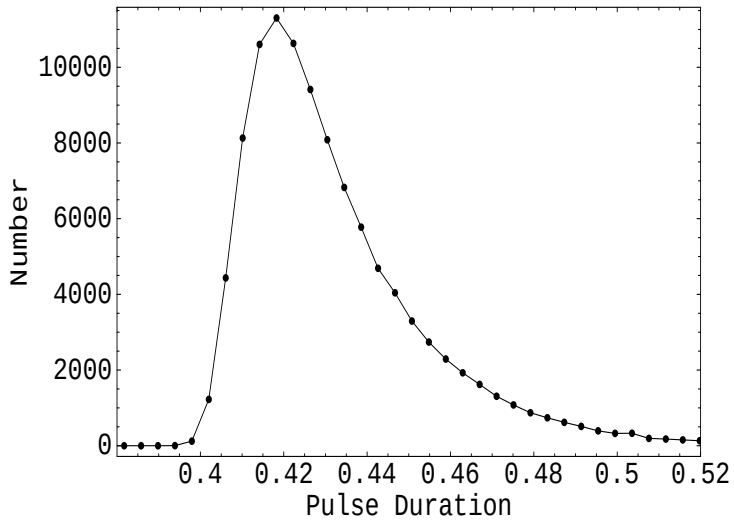

FIG. 7. *Histogram of number of pulses vs. pulse duration in milliseconds for random noise every timestep.*

in Figure 7 for a total of approximately 100,000 pulses with noise added every timestep. The exponential decay (above a threshold) of the number of pulses with increasing pulse duration agrees qualitatively with experimental data.

Statistics for simulations with noise ranging from every timestep (with $\Delta t = 0.01$) to every hundredth timestep are very similar. At a frequency of adding noise every thousandth timestep there is a qualitative change in the statistics toward much longer average pulse durations and much more variation in the pulse durations and separations (see Table 1). The table presents the three qualitatively different regimes of current pulse behavior that we observed in our numerical simulations. The computed solution with noise added every timestep is close to periodic, since with noise every

TABLE 1

Average pulse duration Δt_P in milliseconds and number of pulses for a sample of 250 seconds with different average frequencies of adding noise.

Average frequency	Δt_P	*Number of pulses*
1	0.4	105000
1/1000	1.3	63000
1/10000	8.8	14000

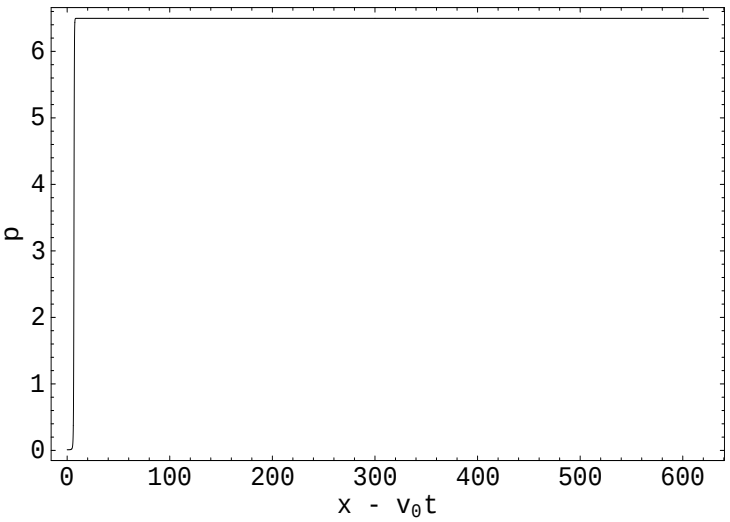

FIG. 8. *Solution $p/\overline{p}$ vs. $(x - v_0 t)\overline{E}/\alpha$ without noise, illustrating that the solution without noise gets stuck at a fixed point.*

timestep the solution cannot get stuck for long at the heteroclinic points. With less frequent noise, the solution may get stuck at a fixed point for a very long time. The elongation of pulse duration with more widely dispersed noise demonstrates convergence to the deterministic case ($\sigma = 0$) in Figure 8. Note that for the "baseline" solution with noise every timestep the length of an orbit is about 6000 Δt. We thus expect a phase transition in the behavior of solutions as the frequency of noise falls below once per baseline orbit. It is possible that the two phases may correspond to the two qualitatively distinct forms of gating ("activation" and "inactivation") experimentally observed in most ionic channels [1].

4. Connection to physical parameter values. We consider here the flow of K^+ ions through a channel of diameter 7 Å and length 10 Å. K^+ channels play a central role in electrical signaling in the nervous system. A typical nerve cell has hundreds of thousands of K^+ channels. For the K^+ channel, the dielectric constant ϵ is on the order of 20, the mobility coefficient $\mu \approx 6 \times 10^{-5}$ cm^2/(V s), and the diffusion coefficient $D \approx 1.5 \times 10^{-6}$ cm^2/s. Note that the Einstein relation holds: $eD/\mu = kT_0 = \alpha$, and that in our units $e^2 = 1.80955 \times 10^{-6}$ eV cm.

Only the current $I \sim 1$–10 picoamperes and the average duration of a current pulse $\Delta t_P \sim 1$–10 milliseconds are directly measurable experimentally. The relationships between the microscopic parameters $\overline{p}$, $\overline{E}$, v_0, and c and the macroscopic parameters

I and Δt_P in our model are as follows:

$$I = (6.5\overline{p})\mu\overline{E}A_C, \quad \Delta t_P = \frac{10\alpha e}{\mu\overline{E}^2}, \quad v_0 = \mu\overline{E}/e, \quad c = \frac{\epsilon\overline{E}^2}{\alpha e^2\overline{p}}. \tag{19}$$

The magic numbers 6.5 and 10 in the formulas for I and Δt_P, respectively, come from the simulation results in Figures 3, 5, and 6: $p_{max} \approx 6.5\overline{p}$ for all cases and $\Delta\tau_P \approx 10/\overline{E}$ for the baseline case of noise every timestep.

The simulations presented above thus represent a range of physical values for I, Δt_P, v_0, p, N, E, and c. A physically natural magnitude for $\overline{p}$ would be a unit charge e spread uniformly throughout the channel volume (2.6×10^{21} cm^{-3}). We choose $\overline{p}$ to be one-half this value so that the average number of ions in the channel when the channel is on is roughly 3.25. We then choose $\overline{E} = 3200$ eV/cm in order to make I equal to 1 picoampere. These values for $\overline{p}$ and $\overline{E}$ yield an average pulse duration of 0.4–8.8 milliseconds (see Table 1). The traveling wave velocity $v_0 = 0.2$ cm/s is the same order of magnitude as the ion permeation velocity v_p through the channel. As expected, $c = 3.5 \times 10^{-6} \ll 1$.

5. Conclusion. It is remarkable that an electrodiffusion model can produce not only rectangular current pulses, but the wide variety of current behavior observed experimentally in channels of biological membranes. It is difficult to get rectangular waves with flat tops from ordinary differential equations. The addition of noise to the drift-diffusion equations can excite a series of heteroclinic orbits with different current pulse durations and separations but equal heights, in accord with experimental measurements of channel currents. Our model serves as an example where nature may make use of ubiquitous thermal noise to accomplish a biological task—in this case turning the channel on and off.

Physical values predicted in the model, like $v_0 \sim v_p$, $\Delta t_P \sim$ 1–10 milliseconds, $\overline{E}$ (implies $|V|_{max} \sim 100$ millivolts), etc., are of the right order of magnitude for biological channels. A conformational change in the protein and the concomitant small charge fluctuations ($c \sim 10^{-6}$) produce gating, rather than a mechanical "flap" or "slider." A small dipolar charge wave (a positive spike followed by a negative spike) turns on the current in the channel, and a similar reversed charge wave (a negative spike followed by a positive spike) turns off the current. The relationship of this charge wave to gating current [1] remains to be investigated in the context of a finite channel with realistic boundary conditions.

Our model depends on concentration through the reference ion density $\overline{p}$. However, $\overline{p}$ is not necessarily coupled to ion densities in the external baths, etc., although it could be. Thus our model can treat both K and Na channels, which are roughly concentration independent, and Ca channels, which are very sensitive to ionic concentrations.

A dynamical systems analysis of the traveling wave solutions is currently in progress. Here we briefly mention three relevant mathematical papers. In [9], Krupa analyzes a robust heteroclinic cycle as an orbit in phase space successively connecting equilibrium points or more general invariant sets (we have a whole line of equilibrium points in our model). The existence of such robust cycles is analyzed in terms of spontaneous symmetry breaking or forced symmetry breaking (possibly induced by stochastic perturbations, as in our model). Stone and Holmes [10] are interested in the creation of structurally stable orbits through random perturbations of an underlying deterministic system. Under such perturbations, they estimate the passage time in heteroclinic orbits from one saddle point to another. Finally, Fiedler, Liebscher, and

Alexander [7] investigate the behavior of solutions to a general system of ordinary differential equations with lines of equilibria under various symmetry assumptions. Techniques from these papers may be applicable to a dynamical systems analysis of our current pulse solutions.

We are currently simulating finite channel effects in the full drift-diffusion model. We have recently reproduced the rectangular current pulses in a 10 Å long voltage biased channel using the full drift-diffusion model. The finite channel simulations are important because the traveling wave pulses have a length equal to $v_0 \Delta t_P \gtrsim 1000$ channel lengths. This is consistent with experimental measurements of current pulses if the ionic velocities are on the order of v_p, since the channel is on for a long time Δt_P compared to an ionic transit time 10 Å$/v_p$. Simulating the full drift-diffusion model will allow us to formulate physically relevant boundary conditions for the finite channel. Simulations using the charge model (10) expressed in terms of the current j

$$\rho(j, E) = -\frac{c}{v_0}(j - \overline{j}) \left| \frac{E}{\overline{E}} - 1 \right|, \tag{20}$$

where $\overline{j} = e v_0 \overline{p}$ produce a nonlinear (sublinear) current-voltage curve, as is observed experimentally (see p. 328 of Hille [1]) and lend credence to the charge model (10). We are also applying our charge model and the current pulse solutions presented here to reproducing "random telegraph noise" current pulses in semiconductor field effect transistors.

REFERENCES

[1] B. Hille, *Ionic Channels of Excitable Membranes*, Sinauer, Sunderland, MA, 1992.

[2] R. S. Eisenberg, M. M. Klosek, and Z. Schuss, *Diffusion as a chemical reaction: Stochastic trajectories between fixed concentrations*, J. Chem. Phys., 102 (1995), pp. 1767–1780.

[3] W. Nonner, D. Chen, and R. S. Eisenberg, *Anomalous mole fraction effect, electrostatics, and binding*, Biophys. J., 74 (1998), pp. 2327–2334.

[4] W. Nonner and R. S. Eisenberg, *Ion permeation and glutamate residues linked by Poisson-Nernst-Planck theory in L-type calcium channels*, Biophys. J., 75 (1998), pp. 1287–1305.

[5] P. Szmolyan, *Traveling waves in GaAs-semiconductors*, Phys. D, 39 (1989), pp. 393–404.

[6] G.-Q. Chen, J. W. Jerome, C.-W. Shu, and D. Wang, *Two-carrier semiconductor device models with geometric structure and symmetry properties*, in Modelling and Computation for Applications in Mathematics, Science, and Engineering, Oxford University Press, Oxford, UK, 1998, pp. 103–140.

[7] B. Fiedler and S. Liebscher, and J. Alexander, *Generic Hopf bifurcation from lines of equilibria without parameters,* I. *Theory,* J. Differential Equations, to appear.

[8] R. P. Feynman, R. B. Leighton, and M. Sands, *The Feynman Lectures on Physics*, Vol. II, Addison-Wesley, Reading, MA, 1964.

[9] M. Krupa, *Robust heteroclinic cycles*, J. Nonlinear Sci., 7 (1997), pp. 129–176.

[10] E. Stone and P. Holmes, *Random perturbations of heteroclinic attractors*, SIAM J. Appl. Math., 50 (1990), pp. 726–743.